Hall mobility of electrons in liquid xenon

1992 J. Phys.: Condens. Matter 4 6055

(http://iopscience.iop.org/0953-8984/4/28/007)

J. Phys.: Condens. Matter 4 (1992) 6055–6072. Printed in the UK

Hall mobility of electrons in liquid xenon

G Ascarelli
Physics Department, Purdue University West Lafayette, IN 47907, USA

Received 10 December 1991, in final form 5 March 1992

Abstract. This communication reports the Hall mobility of electrons injected into liquid xenon whose thermodynamic state is varied along the liquid–vapour coexistence line from the triple point to 272 K. Contrary to what would be expected from transport theory, when $\omega_c \tau < 1$, the Hall angle is not a linear function of the magnetic field. This is particularly important near the mobility maximum, and is interpreted as arising from interference effects. Their importance is a consequence of the fact that, to first order, at the mobility maximum, the electron–phonon interaction is zero while elastic scattering by large density fluctuations persists. Hot electron effects support this interpretation. Beyond 272 K no Hall signal could be detected. Although this is an indication that hopping conductivity is dominant, it is shown that the eventual localized states cannot be associated with electrons trapped into density fluctuations associated with the pure fluid.

1. Introduction

In the course of this paper, we would like to report measurements of the Hall mobility of electrons injected into liquid xenon. A brief report on these measurements appeared previously in the form of a letter [1]; the present paper expands the previous communication.

Measurements of the mobility of electrons injected into insulating liquids have been carried out during the last 30 years on a variety of liquids [2]. Despite the extensive experimental data, the first model that appeared to represent reasonably well the experimental results in the case of rare-gas liquids was published only a little over a decade ago [3]. This model pointed out that density fluctuations would give rise to fluctuations of the energy of the conduction band. The coupling of the electron with the Fourier components of the density fluctuations was thereafter calculated following a formalism that paralleled the calculation of the phonon-limited mobility in either metals or semiconductors. Another related predecessor of similar ideas is the theory of critical opalescence.

The Basak and Cohen theory [3], just like the theory of critical opalescence, predicts an infinite scattering in the vicinity of the critical point that is the result of the divergence of the isothermal compressibility. Experiment instead does not indicate that the electron mobility is zero near the critical point.

Ascarelli [4] modified the Basak and Cohen theory. It was realized that, on account of the much shorter wavelength of the electrons compared to that of visible light, there would be the possibility of large density fluctuations in volumes of the order of half an electron wavelength that could not be well represented by the series

0953-8984/92/286055+18$04.50

expansion used by Basak and Cohen. Furthermore, density fluctuations must remain finite; it is impossible to have either a negative density or a density larger than the close-packed solid. This was sufficient to remove the infinite scattering that appeared in the linear theory.

Large localized density fluctuations must disappear (and be created) slowly compared to the time it would take for a sound wave to propagate a distance equal to its largest dimension. The thermal velocity of electrons is large compared to the velocity of sound; therefore from our point of view, these density fluctuations are static, and they scatter electrons elastically. This is reminiscent of the negligible recoil energy imparted to a Mössbauer nucleus embedded in a lattice.

Scattering associated with small density fluctuations described by phonons clearly remains and must be added to that due to the static ones. Phonon scattering can be treated in the same way as in the case of semiconductors; it is inelastic.

A central assumption of all of the above models is that the electron can be described by a plane wave (or at the most by a Bloch-like wave), i.e. that hopping (or tunnelling, thermally activated or not) between localized states in the tail of the conduction band does not dominate transport.

Symmetry considerations allow the coexistence of localized and delocalized states in a disordered material like a liquid. The predominance of one type of states over the other will depend on details of the potential experienced by the electrons. This potential is a sensitive function of the atomic (or molecular) density. This is exemplified by two recent calculations [5, 6]. In one of these [5] the position of the conduction band with respect to vacuum, V_0, is calculated based on a percolation model: electrons whose energy is above the threshold for the 'lakes to ocean' transition are in the conduction band, those below are in localized states. There is excellent agreement between the measured [7] and the calculated value of V_0 in the case of Xe, not as good in the case of Kr and Ar. The other calculation [6] is instead carried out in the framework of the path integral calculations for the polaron [8, 9] and, depending on the choice of how to describe the wavenumber dependence of the isothermal compressibility, the authors [6] find localized states in Xe in the immediate vicinity of the critical point.

It is appropriate to point out that other successful calculations of V_0 exist based on both the path integral method [10] and a pseudo-crystal approximation [11].

The experimental values of V_0 are [7] such that, over the range of densities characteristic of liquid xenon, V_0 changes by about 0.1 eV. Therefore this is the maximum possible value of a potential well associated with a density fluctuation where the electron could be trapped. In order to have non-zero binding energy, the well of depth ΔV_0 must have a radius R larger than [12]

$$R^2 = \frac{\pi^2 \hbar^2}{8m^* \Delta V_0}. \tag{1}$$

Taking for m^* the experimental value of the effective mass [13], $0.27m_0$*, the value of R equals 17.7 Å. It will have to be increased significantly before an electron will have a binding energy near $k_B T$.

These large density fluctuations are only present in reasonable concentrations, very close to the critical point. They can only have a significant effect on transport properties when their concentration is large compared with the electron density and when their separation is small enough for an electron to tunnel between them. The

magnetotransport contribution of the tunnelling current is in general much smaller than that arising from the more traditional contribution [14, 15], and for holes it may even have the same sign as for electrons!

Another form of localized state is possible in which the electron is elastically scattered by distinct density fluctuations and eventually returns to its point of departure. The multiply scattered waves may then interfere constructively and give rise to something that has some characteristics of a bound state.

This phenomenon is what is labelled weak localization and has been the focus of intensive studies in metals [16, 17]. In solids it is revealed by anomalies of the magnetoresistance that are particularly detectable in the two-dimensional case, i.e. thin films. Other kinds of waves, e.g. photons, show a similar behaviour [18].

2. Sample purification and sample cell

The manufacturer's analysis of the xenon gas indicated < 0.3 ppm O_2, < 2.0 ppm N_2, < 0.9 ppm H_2O, < 1 ppm CO_2, < 0.1 ppm hydrocarbons and < 3 ppm for the combination of Kr, H_2 and Ar.

The gas was further purified by slowly passing it several times over pellets of getter alloy [19] ST707 held at approximately 400 °C in a stainless steel system whose base pressure was approximately 1×10^{-10} Torr when the getter was hot.

The remaining steps in the purification are similar to those used in the case of Ar [20].

The configuration of the sample cell was identical to that used in the case of argon except for the fact that the outer alumina plate, supporting one of the plates of the capacitor used for measuring the dielectric constant, was metallized on both faces. The outer face, which was electrically insulated from the inner one that made up one of the plates of the capacitor, was grounded, so as to decrease the changes of stray capacitance associated with the motion of the assembly inside its stainless-steel container. Except where indicated, the measurement technique was the same as in the case of argon [20].

The temperature was measured by means of a 100 Ω platinum resistance thermometer [21] immersed in the liquid just below the resistive plates and connected in the four-wire configuration. The thermometer current was 0.1 mA. Reversal of the thermometer current was used to cancel the unavoidable thermoelectric voltages that develop at the wire junctions.

The temperature dependence of the resistivity of platinum is given by the Callendar–Van Duren equation [21, 22] whose coefficients are given by the manufacturer [21]. Only one quantity is necessary to calibrate an individual resistor: the resistance at 0 °C. After the calibration was established it was checked by measuring the triple point of xenon. The measured temperature was 0.23 K too high. This constitutes an uncorrected systematic error that decreases towards zero at 0 °C. Extrapolated to the critical point, where its importance would be the largest, it gives rise to an error of 0.04 K.

Electron–hole pairs were created by an x-ray beam produced by 4 MeV electrons from a linear accelerator that are stopped in a lead foil. The radiation is collimated by a $1.7 \times 4 \times 240$ mm^3 tube. This collimator is narrower than that used in the case of argon [20]. As a result the Pb target was in a region inside the yoke of the magnet where the magnetic field did not saturate as readily as in the case of argon. No

deviation of the electron beam was noticed up to when the magnetic field between the pole pieces was well beyond 1.2 T.

The repetition rate of the ionizing pulses was kept at 4 s^{-1} and the electron density that was produced by each pulse of the accelerator was between 10^8 cm and 10^9 cm^{-3} over a volume $1.7 \times 4 \times 10$ mm^3 It was checked that changing the repetition rate to either 0.9 or 7.5 s^{-1} did not affect the experimental results. This is an indication that no free charges remained from one pulse to the next. The absence of a signal just before the x-ray pulse gave further confirmation of this conclusion.

From the measurement of both temperature and pressure, the density can be calculated using an equation of state; several authors have fitted experimental data to an algebraic expression suitable for computer calculations [23–26]. Up to 240 K the saturated vapour pressure equation given by Theeuwes and Bearman [25] is indistinguishable from that of Juza and Sifner [23] but above this temperature the equation given by the latter appears to be in better accord with the experimental data and was used up to 275 K. The density was calculated using the expression given by Street *et al* [24].

An independent measurement of the density of the fluid was obtained from the measurement of the dielectric constant and the application of the Clausius–Mossotti relation. Alternatively, this could be used with the density data from the equation of state, to obtain the polarizability of liquid xenon. Using the latter we find that the density-independent Clausius–Mossotti (CM) function is: $CM=(10.05 \pm 0.02) \times 10^{-3}$ l mol^{-1}, in excellent agreement with previous measurements [27, 28].

The temperature of the sample cell, and the temperature gradient along the stainless-steel tube that supports it, were independently controlled by means of three separate heaters whose temperature control systems had separate thermistors as sensors in the feedback loop. The temperature along the stainless-steel tube was measured by means of copper–constantan thermocouples. To improve the thermal contact between the thermocouples and the outside wall of the stainless-steel tube, they were indium soldered to it.

To decrease the heat exchange between the sample cell and the liquid-nitrogen bath, the sample cell and the supporting tube were wrapped in aluminized mylar and enclosed in another tube immersed in liquid nitrogen, that in turn was evacuated to about 10^{-2} Torr, a pressure low enough to ensure that the main mechanism for heat exchange was radiative. This prevented a temperature inversion and decreased very much the current that had to be supplied to each heater. As an example, near the triple point, the electrical power into the two lowest heaters was of the order of 5 mW and no power was supplied to the top one. This input power increased to about 50 mW at 270 K.

3. Experimental results

The tangent of the Hall angle was measured between 161.7 K (triple point 161.37 and 272.1 K (critical point 289.734 K) along the liquid–vapour coexistence line. The experimental errors are estimated to be approximately 10% except for the two highest temperatures, where the errors are about twice as large.

Classical Boltzmann transport theory [29] provides an expression for the tangent

of the Hall angle (Θ)

$$\tan\Theta = \frac{E_y}{E_z} = -\frac{D}{A} \tag{2}$$

where

$$A = \left\langle \frac{\tau}{1+(\omega_c\tau)^2} \right\rangle \tag{3}$$

$$D = \left\langle \frac{\omega_c\tau^2}{1+(\omega_c\tau)^2} \right\rangle \tag{4}$$

where τ is an energy-dependent collision time and $\omega_c = eB/m^*$.

In the limit of small ω_c, $\tan\Theta = E_y/E_z = -e(\langle\tau^2\rangle/\langle\tau\rangle)B/m^* = -\mu_H B$ where μ_H is the Hall mobility and B is the magnetic field. The brackets $\langle\ \rangle$ indicate an average over the electron distribution. In the large magnetic field limit when $\omega_c\tau \gg 1$, $\tan\Theta = eB/(m^*\langle 1/\tau\rangle)$. In general these two limits are not equal and we should expect that deviations from a linear dependence of $\tan\Theta$ on B should occur in the region where $\omega_c\tau \simeq \mu_H B \sim 1$. Knowing τ as a function of energy, these deviations can be calculated.

The voltages that produce the fields E_x and E_y are directly measured. The voltage applied to the resistive plates is known and so is their length, from which the corresponding field E_x is calculated. The separation between the resistive plates is known and the voltage that must be applied to balance the effect of the magnetic field is measured (see [20]), from which one obtains E_y.

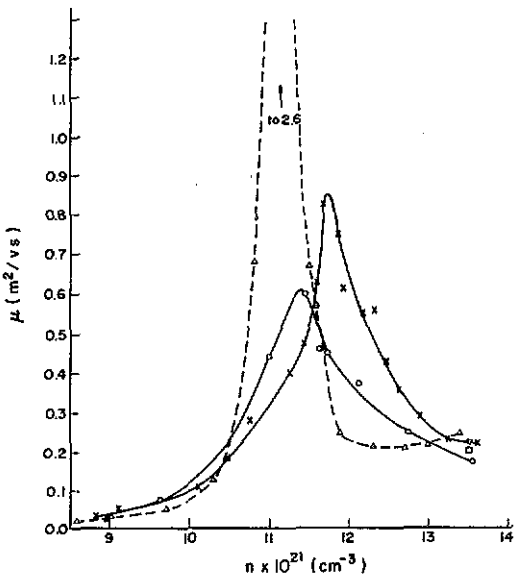

Figure 1. Measured mobility of electrons injected in liquid xenon: (x) Hall mobility, present measurements; (o) TOF mobility [30]; ($\triangle$) model calculation [31]; ($\square$) TOF mobility [49]; (∇) TOF mobility [32]. The curves are drawn as a guide to the eye.

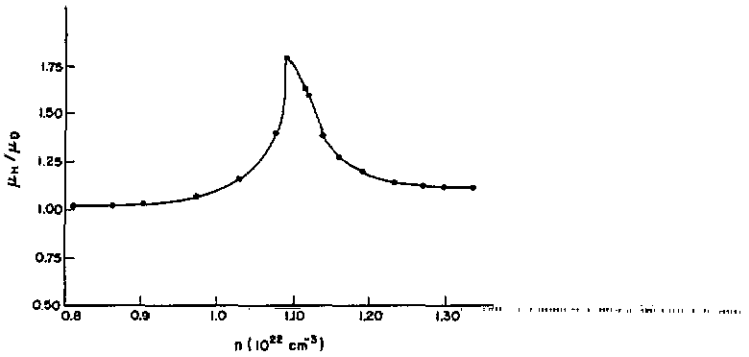

Figure 2. Calculated ratio of the Hall and drift mobilities [31].

The results of the Hall mobility measurements are shown in figure 1. The results of the TOF measurements [30] as well as the results of the mobility calculation [31] are shown in the same figure. All the data refer to electrons in a liquid in equilibrium with its vapour, i.e. along the liquid–vapour coexistence line. The calculation of the ratio of the Hall and the drift mobility is shown in figure 2. The asymmetrical shape of this curve reflects the fact that phonon scattering rapidly dominates the mobility because the velocity of sound rapidly decreases with the approach to the critical point.

The measurements displayed in figure 1 were carried out with electric fields between 1.4 and 3 V cm^{-1} except near 272 K, where a field as high as 4.9 V cm^{-1} was used. Hall mobility measurements using fields as high as 15.8 V cm^{-1} were attempted at 275 K, but no effect of the magnetic field could be detected above 272.1 K.

Examples of the magnetic field dependence of $\tan\Theta$ are shown in figures 3 and 4. As is obvious from the data in figure 3 even at relatively modest electric fields, the mobility is strongly electric-field-dependent. Such a dependence has been observed by others [30, 32]. Although this is assigned to hot electrons, no self-consistent calculation that considered the detailed mechanism for such a non-ohmic response has been carried out.

The main features of these data are the discrepancies between the temperatures (or densities) where the maxima of the TOF and Hall mobilities are found, as well as the differences between the magnitude of the calculated and measured Hall mobility maxima. Finally, possibly the most interesting feature is how the non-linear dependence of $\tan\Theta$ on the magnetic field increases towards the mobility maximum. The disappearance of the Hall signal beyond approximately 272 K while the TOF signal remains observable is an indication of hopping (or tunnelling) transport, whose details remain, however, unclear.

Despite its obvious interest, magnetoresistance could not be measured. Not only it is expected to be of higher order in the magnetic field than the Hall effect, but it would have required either a shorter accelerator pulse and less noise from the discharge of the pulse-forming delay lines, or the addition of wires in the sample cell. Space limited the latter.

4. Interpretation of results

The first discrepancy mentioned in the previous section that we would like to address

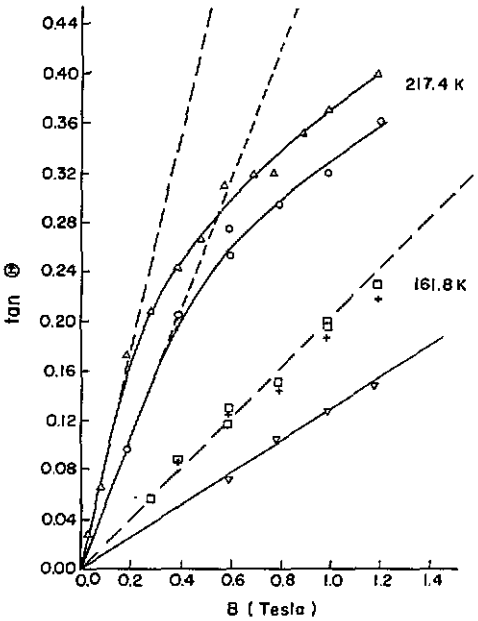

Figure 3. Magnetic field dependence of tan Θ: $T = 161.8$ K, $n = 13.58 \times 10^{21}$ cm^{-3}, (▽) 1.58 V cm^{-1}, (□) 7.77 V cm^{-1}, the small non-linearity in the curve is possibly just beyond the deviation from a straight line that could be expected from experimental error; △: $T = 217.4$ K, $n = 11.69 \times 10^{21}$ cm^{-3}, (△) 1.58 V cm^{-1}, (○) 12.25 V cm^{-1}. The curves through the points are just to be taken as a guide to the eye.

is the lack of coincidence of the density (and temperature) where the maximum found in the Hall mobility and that found in the TOF data are observed [30].

We believe that this difference, that corresponds to 5.5 K, is due to the fact that in [30] the temperature of the liquid was taken as equal to the temperature measured by a thermocouple located on the outer portion of a cell with 1 cm thick glass walls containing the sample. Similar discrepancies were found in the case of argon [20, 33] but disappeared when the Hall mobility data were compared with the TOF mobility data obtained from a sample whose temperature sensor was in better contact with the liquid [34].

A more serious discrepancy is the larger difference of the densities where the experimental and the calculated mobilities peak. The mobility models [3, 4] indicate that the mobility maximum is a consequence of the minimum of V_0; the density of both should therefore coincide. A difference of 15 K is outside the experimental errors.

In argon [20, 33, 34], krypton [35], neopentane [36, 37] and tetramethylsilane [37], where both the mobility and V_0 have been measured as functions of density, the minimum of V_0 is at densities below that corresponding to the mobility maximum. In the case of methane the maximum of the mobility and the minimum of V_0 appear to coincide [38].

This author [20] suggested that the density where V_0 has a minimum, and where μ has a maximum, do not coincide because the average density of the fluid is lower than that in the immediate vicinity of the photocathode used to measure V_0. The

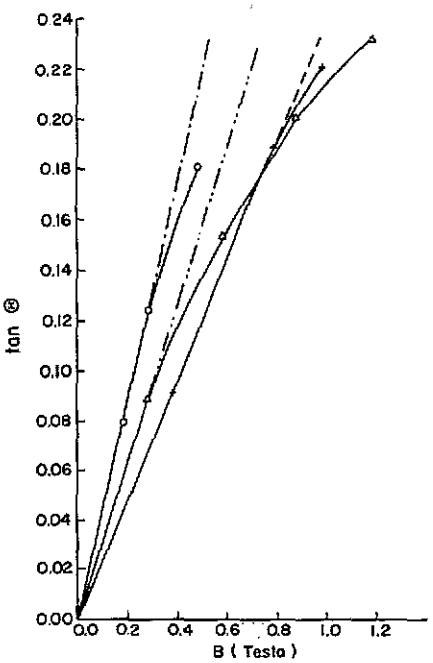

Figure 4. Magnetic field dependence of $\tan\Theta$: (o) 196.0 K, 1.25×10^{22} cm^{-3}; (Δ) 183.5 K, 1.29×10^{22} cm^{-3}; (+) 173.1 K, 1.32×10^{22} cm^{-3}. All data were taken with a field of 1.58 V.

cause is that the interaction of an atom with the photocathode is larger than the interaction between two similar atoms. This is the origin of surface tension. The same suggestion was made by De Gennes [39] in connection with the wetting transition and by Israelachvili [40] in connection with the forces acting between two plates separated by a few nanometres. In the case of liquid ammonia, Bennet *et al* [41] indicate that there is a preferred orientation of molecules in the immediate vicinity of a photocathode. Finally, reflecting the fact that V_0 is negative for xenon, scanning tunnelling microscopy [42] indicates a dramatic increase of the tunnelling current in correspondence to the positions where xenon is adsorbed on the metallic surface. This increase in density is due to the polarization of the atoms by the image potential created by their randomly fluctuating electric dipole. It is this interaction [39, 43] between the random dipole associated with the van der Waals forces and its image that is the mechanism that creates an increase of the atomic density next to the surface.

This difference between the density of the fluid next to the photocathode and that of the bulk is not expected to be constant at all densities. It should be largest near the critical point and be small near the triple point, where the density is closest to that of the close-packed solid.

The discrepancy between the magnitude of the calculated and the measured mobilities is likely to have at least two origins.

In the mobility calculation [4, 31], a rough approximation was made when considering the effect of static density fluctuations on the portion of the scattering due to phonons. This is important near the critical point but has a negligible effect near

the mobility maximum of xenon, which is $\simeq T_c/4 \sim 72$ K below the critical point. Here static density fluctuations do not have a large effect on the parameters that determine phonon scattering. By way of contrast, the higher-order term that would describe, for example, the scattering by two phonons was not taken into account in the model calculation [4, 31]. As a result there is likely to be an overestimate of the phonon-limited mobility.

The contribution of other scattering mechanisms beside phonons and static density fluctuations cannot be excluded and there is evidence that they are particularly important near the mobility maximum, where the other scattering mechanisms are small. When the mobility measurements at 217 K were repeated about 4 months after those reported here, the mobility had decreased about 20%. This decrease followed the condensation of the gas in the cylinder attached to the sample cell, which had remained at room temperature for a large fraction of a year.

Based on the analysis of the residual gas with a quadrupole mass spectrometer, the most likely impurities are CO and CO_2 that desorbed from the walls of the system, which remained at room temperature. The rate of desorption can be estimated from the limiting pressure attained before filling the cell with the sample gas.

The cross sections for scattering of electrons by CO_2 and CO in dilute gases [44, 45] are respectively $\simeq 1 \times 10^{-14}$ cm^2 and $\simeq 2 \times 10^{-15}$ cm^2. In order to explain the decrease of the mobility over a period of several months, the required cross section of the scatterers must be about 20 times larger than that of electrons in gaseous CO_2. We do not know how to evaluate if such a cross section is reasonable.

Of all the previously mentioned discrepancies the most interesting are the nonlinear dependence of $\tan\Theta$ on the magnetic field, and the disappearance of the Hall signal above 272 K. Below we will describe an interpretation of the magnetic field dependence along the lines used to describe localization in metals [16, 17], or of light in turbid solutions [18]. The explanation of the electric field dependence of the mobility requires a detailed knowledge of both the energy-loss mechanisms and the electronic density of states (i.e. the equivalent of the energy–momentum relation in the case of a crystal) so that the electron distribution can be evaluated. Neither is available.

4.1. Weak localization

Consider an electron that is repeatedly scattered at positions $r_1, r_2, \ldots, r_N$. The probability that the electron returns to a position r_N such that $r = |r_N - r_1|$ is given by the solution of the diffusion equation, i.e.

$$P(r,t) = \frac{1}{(4\pi Dt)^{3/2}} \exp\left(-\frac{r^2}{4Dt}\right) \tag{5}$$

where $P(r,t)$ is the probability that after a time t the electron ends up a distance r from its starting position. D is the diffusion coefficient of the electron.

The electron is not, however, a classical particle. The resulting scattered wave will have a probability density that is not isotropic even if the individual scattering events at $r_1, \ldots, r_N$ are isotropic because the waves scattered at r_1 and r_N interfere (just like in the case of the optical double-slit experiment). The square of the scattered probability amplitude is proportional to $\cos^2 \delta/2$ where δ is the phase difference of the waves scattered at r_1 and r_N. Such an interference is only possible if the waves

scattered at r_1 and r_N are coherent, i.e. all the scattering events at $r_1, \ldots, r_N$ are elastic.

In the above description the scattering from r_1 to r_N has been treated differently from that taking place in the reverse order. Symmetry can be restored, and the results are unchanged, if we consider the phase difference of the wave scattered from r_1 to r_N and that scattered in the reversed order from r_N to r_1.

The total path length from r_1 to r_N is limited by the condition that all the scattering be elastic and its most probable length is equal to the inelastic mean free path L. By way of contrast, the average between the elastic scattering events is the elastic mean free path Λ, which also determines the diffusion constant D when $L \gg \Lambda$.

Despite the fact that the electron is not a classical particle, the correspondence principle assures that the average probability that the electron returns to the vicinity of the origin can be approximately calculated classically using the diffusion equation.

For particles of velocity v, $t = L/v$ and $D = v\Lambda/3$. Inserting in the expression for $\langle r^2 \rangle = 6Dt$ one finds $\langle r^2 \rangle = 2L\Lambda$. In the case of either metals [16, 17] at low temperature or light [18], $L \gg \Lambda$, the ratio L/Λ reaches a few thousand.

The phase difference of the waves scattered at r_1 and r_N (figure 5) is given by

$$\delta = (k_f + k_i) \cdot (r_N - r_1) = q \cdot (r_N - r_1). \tag{6}$$

Here k_f and k_i are the wavevectors of the electron after and before scattering.

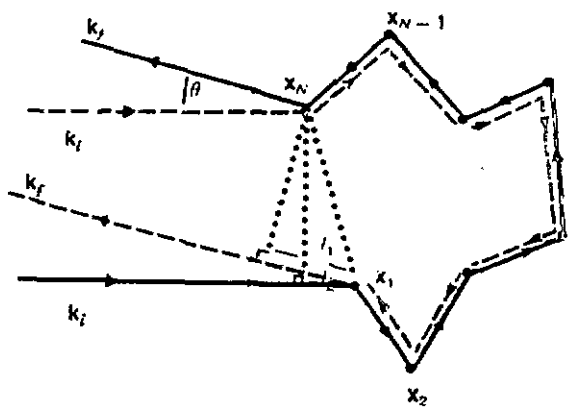

Figure 5. Scattering of an electron from $r_1, r_2, \ldots, r_N$. The path difference of the wave scattered at r_1 and r_N is $l_1 - l_2$.

In the backward direction, electrons of all momenta interfere constructively, just as in the corresponding case for light. The width of the interference pattern will, however, depend on the momentum of the electrons since $q = 2k \sin(\theta/2)$. Here θ is the scattering angle (figure 5). The first minimum of the interference pattern will occur when $q \cdot (r_N - r_1) = \pi$.

It is clear that if we wish that the width of the first interference maximum will correspond to a large value of θ we must have

$$|q| \simeq |k| \simeq \frac{1}{|r_N - r_1|}. \tag{7}$$

This will assure that a large fraction of the electrons of wavevector $|k|$ will contribute to the interference maximum, or alternatively that, for these electrons, there is a large range of angles between q and $(r_N - r_1)$.

When $|k| \gg |r_N - r_1|^{-1}$, few electrons contribute to the interference maximum because the range of angles θ within the central interference maximum is small. In the case of xenon $|r_N - r_1|$ is of the order [31] of 8×10^3 Å and the corresponding energy $\hbar^2/2(r_N - r_1)^2 m^*$ is far below $k_B T$.

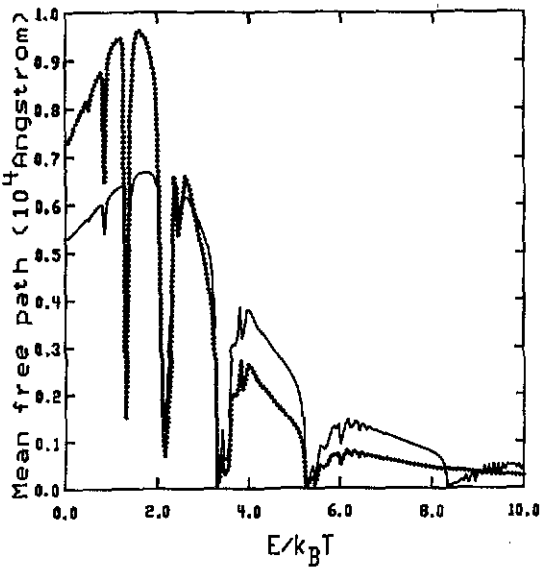

Figure 6. Elastic mean free path Λ as a function of electron energy near the calculated mobility maximum (230.0 K, $n = 1.121 \times 10^{22}$ cm^{-3}). The smallest volume for the density fluctuation that is considered has on average 256 atoms (dotted curve) or 128 atoms (full curve). The calculation quoted in the text corresponds to the case when the smallest volume where the density fluctuation takes place has 256 atoms [31]. The sharp peaks that appear in the figure are a consequence of resonances produced by the square wells used to describe the potential associated with density fluctuations.

In figure 6 we plot the electron mean free path due to scattering by *static density fluctuations* as a function of electron energy corresponding to a temperature in the vicinity of the *calculated* mobility maximum. This curve is obtained using the same computer program used in [31]. As pointed out in this reference, the sharp *resonances* are the consequence of the fact that the static density fluctuations were considered to have sharp edges and thus give rise to square wells and barriers. It is the energy dependence of the mean free path due to scattering by static density fluctuations, as well as the constant mean free path arising from phonon scattering, that are used in calculating the mobility shown in figure 1, as well as μ_H/μ_d shown in figure 2. The only adjustable parameter in the calculation is the electron effective mass, which is taken as $0.27m_0$ in agreement with the effective mass estimated from exciton spectra [13].

The application of the magnetic field changes the generalized momentum p into $\Pi = (p - eA)$ and modifies the interference condition from $\delta_1 = q \cdot (r_N - r_1) < \pi$

by adding a term

$$\delta_2 = \frac{2}{\hbar}\oint e\boldsymbol{A}\cdot \mathrm{d}\boldsymbol{l} = \frac{2e}{\hbar}\int_S \nabla \times \boldsymbol{A}\cdot \mathrm{d}\boldsymbol{S} = \frac{2e}{\hbar}\Phi_S \tag{8}$$

to the phase. The first integral is taken over the path $r_1,\ldots,r_N,r_1$ and the factor 2 arises because the phase of the wave travelling in the clockwise direction increases while that of the wave travelling in the anticlockwise direction decreases by the same amount (figure 5). The quantity Φ_S is the flux of the magnetic field through the area bounded by the path $r_1,\ldots,r_N,r_1$. This area may be estimated as not larger than that of a circle whose circumference is L. The condition that many electrons can contribute to the interference is that

$$|(\hbar\boldsymbol{k} - e\boldsymbol{A})| = |\hbar\boldsymbol{k}_0| \sim \frac{\hbar}{|(\boldsymbol{r}_N - \boldsymbol{r}_1)|} \tag{9}$$

where $\hbar k_0$ clearly corresponds to a small momentum. This equation implies that when the magnetic field is increased (and therefore A is increased) the magnetic field sweeps electrons of increasing momentum into the interference condition. These electrons do not contribute to transport.

Such effects are unimportant in metals because the state of the electrons we are considering is always very much below the Fermi energy and therefore they do not contribute to transport phenomena. In the case of metals, L/Λ is large ($\simeq 1000$) and the flux of the magnetic field through each one of the many possible virtual paths followed by the electron gives a different contribution to the phase shift of the scattered wave, thus cancelling any interference effect. In the present case, this ratio is only of the order of 5 and the number of equivalent paths is thus small.

Since $\hbar k_0$ is small we will commit only a small error if we consider that the electrons that give rise to the interference are centred around $p = eA$ and that they represent a fraction of the total number of electrons of that momentum, i.e. that

$$\Delta N = Cp^2\left[\exp\left(-\frac{p^2}{2m^*k_BT}\right)\right]\Delta p \tag{10}$$

electrons do not contribute to transport.

We must now calculate $\tan\Theta$ using the electron distribution that has the 'hole' described by the above equation. Equation (2) becomes

$$\tan\Theta = \left\{\left\langle\frac{\omega_c\tau^2}{1+(\omega_c\tau)^2}\right\rangle - C\left(\frac{\omega_c\tau^2}{1+(\omega_c\tau)^2}\right)\left[\exp\left(-\frac{p^2}{2m^*k_BT}\right)\right]p^4\Delta p\right\}$$
$$\times\left\{\left\langle\frac{\tau}{1+(\omega_c\tau)^2}\right\rangle - C\left(\frac{\tau}{1+(\omega_c\tau)^2}\right)\left[\exp\left(-\frac{p^2}{2m^*k_BT}\right)\right]p^4\Delta p\right\}^{-1}. \tag{11}$$

An additional factor p^2 appears in this equation because the calculation of $\tan\Theta$ arises from the ratio of the calculations of two currents and, according to the Boltzmann equation, there will be two factors p, one arising from the velocity of the carriers and the other from the term $\delta f_0/\delta p$ where f_0 is the equilibrium Boltzmann distribution. The factor C hides the integration over angle variables, while the range

of momenta Δp is in part connected to the direction of incidence of the electrons with respect $r_1 - r_N$ and in part reflects the fact that the separation between these scatterers is not uniform. In principle an integration over all momenta should be carried out. What is being done instead is considering a 'hole' in the electron distribution as if it could be replaced by one with infinite steep walls and width Δp so that $p\Delta p/m^*$ is small compared to $k_B T$.

Expanding the above equation for $\tan\Theta$ in series and keeping only the terms linear in Δp one finds

$$\tan\Theta = \tan\Theta_0 + Cp^4(\omega_c\tau - \tan\Theta_0)\frac{\tau/1 + (\omega_c\tau)^2}{(\tau/1 + (\omega_c\tau)^2)} \times \left[\exp\left(-\frac{p^2}{2m^* k_B T}\right)\right]\Delta p. \tag{12}$$

In this expression $\tan\Theta_0$ is the value of $\tan\Theta$ that would be observed in the absence of this interference phenomenon.

We can now introduce the fact that $|p - eA| \simeq |p_0|$ where p_0 is small, i.e. we can write $[p\cdot(r_N - r_1)]^2 \simeq (e\Phi_S)^2$. For a fixed $|p|$ the average of the left-hand side of this equation is $(1/3)p^2(2L\Lambda)$. The average of the right-hand side of the equation is $4e^2B^2S^2/3$, where S is the area enclosed by the path $r_1, \ldots, r_N, r_1$. As pointed out earlier the upper limit for S is the area of the circle whose circumference is L, i.e. $S = L^2/4\pi$. Substituting in the expression for $\tan\Theta$ one finds

$$\Delta = \tan\Theta_0 - \tan\Theta \propto B^4 \exp\left\{-\left[\frac{e^2}{16\pi^2 m^* k_B T_e}\left(\frac{L^3}{\Lambda}\right)B^2\right]\right\}. \tag{13}$$

This expression predicts that $\log(\Delta/B^4)$ should be proportional to B^2/T_e provided neither $\log\{(\tau/[1+(\omega_c\tau)^2]\}$ nor L^3/Λ is a rapidly varying function of energy. T_e is the electron temperature that characterizes a Maxwellian distribution. In the case when the applied electric field is sufficiently small, the electron temperature is equal to the temperature of the liquid.

In figure 7 the data of figure 3 are plotted so as to test whether the expression for Δ is a good representation of the experimental data. It was assumed that $\tan\Theta_0$ varied linearly with B and the slope was assumed equal to the observed value at low magnetic field. The calculated mean free path associated with the scattering by the static density fluctuations [31] near the mobility maximum is shown in figure 6; the phonon-limited mean free path L is well known to be independent of the energy of the electrons provided the non-equilibrium phonon distribution (in the case of hot electrons) can be neglected. This appears reasonable on account of the small electron density.

The plot in figure 7, corresponding to the data taken with a 12.25 V cm^{-1} field, shows that, in the case of warm electrons, the form of Δ is consistent with that expected from a Maxwellian distribution. From the slope of the straight line the warm electron temperature appears to have increased a factor $\simeq 3$ above the temperature of the liquid while the electron mobility (obtained from the $\tan\Theta$ versus B plot when $B \to 0$) is decreased by $4772/8348 \simeq 3^{1/2}$ (more digits were kept in this ratio than is warranted by the accuracy of the measurements).

These results must, however, be taken with caution on account of the paucity of data and the experimental errors, which could easily mask either a deviation of

the warm electron distribution from a Maxwell–Boltzmann distribution or the energy dependence of other parameters, e.g. m^*, L or Λ.

Another type of comparison can be made between the experimental data and the model calculation by comparing the value of L^3/Λ obtained from the slope of the low-field data in figure 7 ($L^3/\Lambda = 4 \times 10^8$ Å^2) and the value calculated [31]: $L^3/\Lambda = 8 \times 10^9$ Å^2.

Considering all the approximations made in the course of the calculation, the agreement is astonishingly good.

It is worth while to point out that the present analysis for xenon can also be applied to argon near the mobility maximum. At the time [20] was published, the non-linear dependence of $\tan\Theta$ on the magnetic field was puzzling. A plot of these data, using the same variables as in figure 7 is shown in figure 8. The agreement between the calculated and the experimental values of L^3/Λ is comparable to that in the case of xenon. The value of Δ is significantly smaller than in the case of xenon and the number of data points is extremely small. For these reasons, a note of caution was expressed by the author when this interpretation was initially presented [46].

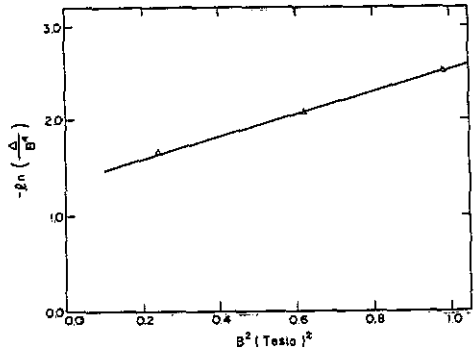

Figure 7. Data from $\tan\Theta$ for liquid argon near the mobility maximum [20] plotted so as to test the form of equation (14).

Before concluding this section it is appropriate to point out that the same form of relation between $\log(\Delta/B^4)$ and $(L^3/\Lambda)(B^2/T)$ could be obtained using a slightly different model.

When an electron scattered from r_1 to r_N and back to r_1 experiences a phase shift of $2\pi n$ (n an integer), this corresponds to having a bound state. Again for low values of n the electron momentum (p_0) must be such that $p_0^2/2m^* \ll k_B T$. The application of the magnetic field introduces a phase shift $e\Phi_S/\hbar$. In order to maintain the resonance condition the value of p must increase so that $|(p - eA)| = |p_0|$. The remaining reasoning follows exactly the same lines as before. The only difference in the result will be a decrease of the numerical coefficient multiplying $(L^3/\Lambda)(B^2/T)$ by a factor of about 40.

On account of the numerous approximations that have been made, as well as the fact that the measured Hall mobility is about three times smaller than the calculated one, it is difficult to decide whether one model is in significantly better agreement with experiment than the other.

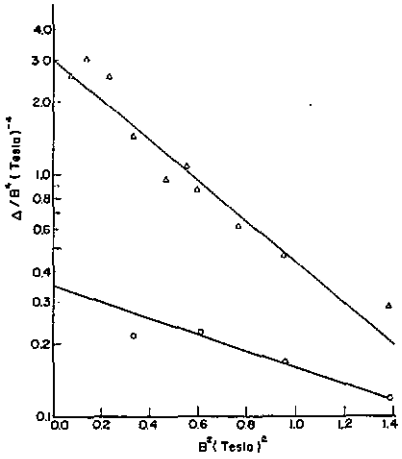

Figure 8. Data from figure 3 near the mobility maximum plotted according to the predictions of equation (14). The detailed form of the magnetic field dependence of $\tan\Theta_0$ above about 1 T depends on the energy dependence of the collision time. On account of the uncertainties a linear dependence was chosen. Using the calculated values of $\tan\Theta$ at 230.0 K, the deviations from a linear behaviour would have been less than 10% at 1.2 T. (△), electric field 1.4 V cm^{-1}, (○), electric field 12.25 V cm^{-1}. The temperature is 217.4 K in both cases.

4.2. Hopping conductivity

It was pointed out earlier that no Hall signal could be observed above 272 K, even though a signal associated with the electrical conductivity was clearly detectable both in this study as well as in the TOF measurements [30]. Attempts to detect a Hall signal at 276 K gave a signal at least about five times lower than at 272 K and in the noise.

Usually the absence of a Hall signal, or a Hall signal that is small compared with what one would expect from the mobility, is considered as the signature of the hopping or tunnelling (thermally activated or not) regime. The reason is that, in order to observe a Hall signal, there must be a 'side' jump, and this implies that the electron must be shared by three sites rather than two, as is necessary in order to observe conductivity [14, 15].

In the case of xenon [30] it had previously been reported that an increase of the applied field above 10 V cm^{-1} was necessary to observe a TOF signal. This behaviour was termed quasi-localization. It was surmized that such a behaviour implied that the electron was being temporarily excited from a localized state into the conduction band. If so, during its residence in the conduction band, the electron would contribute to the Hall signal.

An example of two cases of ionic conductivity, where the ion mobilities are almost the same, and where the 'collision times' are close to the electron collision time in xenon near 270 K, is provided by interstitial silver in AgBr and AgI. A study of the magnetoconductivity was carried out [47] and a Hall signal was only found in the super ionic conductor AgI. Liou *et al* [47] suggest that the reason is that transport in AgI should be visualized as a correlated motion of the Ag ion, while in the case of AgBr the 'jumps' of the Ag ions are uncorrelated.

A similar consideration should apply to the electronic case if the tunnelling probability between two sites is sufficiently small so that the probability that the electron

be shared between three non-collinear sites can be neglected.

We wish to examine if it is reasonable to expect that hopping takes place between states localized in density fluctuations created in pure xenon at $\simeq 275$ K.

The probability that a density fluctuation whose value is $\Delta n \pm \mathrm{d}\Delta n$ is found around a density $\overline{n}$ in a volume Ω is

$$P(\overline{n}, \Delta n)\,\mathrm{d}\Delta n = \left(\frac{\Omega}{2\overline{n}\pi S(0)}\right)^{1/2} \left[\exp\left(-\frac{\Omega(\Delta n)^2}{2\overline{n}S(0)}\right)\right] \mathrm{d}\Delta n \qquad (14)$$

where $S(0) = \overline{n}\chi_T T$, χ_T being the isothermal compressibility.

The largest possible depth ΔV_0 of an attractive square well is when Δn corresponds to the difference between $V_0(\overline{n})$ ($\overline{n} = 8.65 \times 10^{-3}$ Å^{-3} at 275 K) and $V_0(n_{\min})$ ($n_{\min} \simeq 1.164 \times 10^{-2}$ Å^3 at 217.4 K). The first bound state (with zero binding energy) arises when the radius of the well is $R^2 = (\pi^2\hbar^2)/(8m^*\Delta V_0)$; $R \simeq 17.7$ Å when $m^* = 0.27m_0$. The binding energy ($\Delta V_0 = 0.1$ eV $\simeq k_B T$ when $R = 27$ Å, a density fluctuation whose diameter is much larger than the potential wells that affect the mobility calculation. The density of such wells is

$$N = \left(\frac{1}{2\Omega}\right) P(\overline{n}, \Delta n)\,\mathrm{d}\Delta n. \qquad (15)$$

The additional factor 2 arises because the probability of a density fluctuation with a positive and a negative value of Δn are the same.

Taking $S(0) = 1.086$, $\Delta n = 3 \times 10^{-3}$ Å^{-2} and $\mathrm{d}\Delta n = \Delta n/10$, N is about 10 cm^{-3}! It is difficult to envisage how such a small concentration of density fluctuations could be significant, particularly when the electron density is many orders of magnitude larger.

An extrinsic mechanism, that may eventually favour the formation of density fluctuations where the electron is trapped, appears as a more likely explanation for the observations. Intrinsic density fluctuations will become significant within about 1% of T_c, rather than the 5% that is being considered here. With a suitable choice of $\chi(q)$ the theoretical calculation by Hsu and Chandler [6] reaches a similar conclusion.

5. Conclusions

The Hall data presented in this paper are consistent with the previous TOF data [30] as well as with the previous mobility calculation [31]. They support both the estimate of the electron effective mass $\simeq 0.27m_0$ in agreement with recent spectroscopic data [13], as well as the idea that the motion of the electron can be approximated by a plane wave scattered primarily by phonons and by large, basically static density fluctuations.

Two new features of the mobility have been found. Near the mobility maximum where $\mathrm{d}V_0/\mathrm{d}n = 0$, most of the scattering is elastic and the coherence length of the electron becomes long in comparison with the elastic mean free path. In these conditions interference effects become important and are revealed in the magnetoconductivity. Contrary to what happens in metals, the magnetic field does not wash out all traces of this interference because the waves that contribute to the interference pattern can follow only a very limited number of paths and low values of momenta contribute to transport in a non-degenerate electron gas.

In the model calculation used to explain the non-linear dependence of the tangent of the Hall angle on the magnetic field, we considered the interference of an electron wave associated with scattering centres located in a particular region of space whose dimension is of the order of L^3. If one should have averaged over all the phase shifts that exist over the whole sample, the interference pattern would be washed out. This is the same kind of problem as when a light beam incident on a glass plate gives rise to interference fringes: fringes will be seen when the thickness of the plate does not change significantly compared with a wavelength of the light over the volume traversed by the light beam. One may wonder if the same phenomenon is not connected with the different result that is obtained when one considers an average over the canonical and the grand canonical ensemble [48].

The Hall signal could not be observed above 272 K while a TOF signal persisted. This is an indication of hopping conductivity in which the electron tunnels from one localized state to another. However, the density of such states that may be expected in the pure liquid, assuming a square-well potential and the applicability of the effective-mass approximation, is several orders of magnitude too small to make such an explanation plausible. Therefore the observation of hopping conductivity is unlikely to indicate an intrinsic effect at a temperature 5% below the critical point. It is instead more likely to be associated with impurities that may provide both the localized states, as well as favor the formation of density fluctuations. The identification of these impurities is, however, lacking.

Acknowledgments

I would like to thank Professors G Giuliani, P Muzikar, H Nakanishi and L L Van Zandt for illuminating discussions.

References

[1] Ascarelli G 1991 *Phys. Rev. Lett.* **66** 1906
[2] Schmidt W F 1977 *Can. J. Chem.* **55** 2197
[3] Basak S and Cohen M H 1979 *Phys. Rev.* B **20** 3404
[4] Ascarelli G 1986 *Phys. Rev.* B **33** 5825
[5] Simon S H, Dobrosavljevic V and Stratt R M 1991 *J. Chem. Phys.* **94** 7360
[6] Hsu D and Chandler D 1990 *J. Chem. Phys.* **93** 5075
[7] Reininger R, Asaf U, Steinberger I T and Basak S 1983 *Phys. Rev.* B **28** 4426
[8] Feynman R P 1955 *Phys. Rev.* **97** 660
[9] Feynman R P, Hellwarth R W , Iddings C K and Platzman P M 1962 *Phys. Rev.* **127** 1004
[10] Lopez-Castillo J M 1990 private communication
Lopez-Castillo J M, Frongillo Y, Pleukiewicz B and Jay-Gerin J P 1992 *J. Chem. Phys.* at press
[11] Plenkiewitcz B, Jay-Gerin J P, Plenkiewicz P and Bach G B 1986 *Europhys Lett.* **1** 455
[12] Landau L and Lifchitz E 1967 *Mecanique Quantique* (Moscow: Mir) p 135
[13] Reshotko M, Asaf U, Ascarelli G, Reininger R and Steinberger I T 1991 *Phys. Rev.* B **43** 14174
[14] Mott N F and Davis E A 1979 *Electronic Processes in Non Crystalline Materials* (Oxford: Clarendon) p 240
[15] Ehenreich H (chair) 1972 *Fundamentals of Amorphous Semiconductors* Ad Hoc Committee on the Fundamentals of Amorphous Semiconductors, National Academy of Sciences, Washington
[16] Bergman G 1984 *Phys. Rep.* **107** 1
[17] Chakravarty S and Schmid A 1986 *Phys. Rep.* **140** 193
[18] John S 1988 *Comment. Condens. Matter Phys.* **14** 193; 1991 *Phys. Today* May p 32
[19] SAES Getters SpA, Milan, Italy

[20] Ascarelli G 1989 *Phys. Rev.* B **40** 1871
[21] Mod Pt100 Sensing Devices Ltd, Lancaster, PA 17601, USA
[22] Plumb H H, Powell R L, Hall W J and Swindells J F 1972 *American Institute of Physics Handbook* 3rd edn, ed D E Gray (New York: McGraw Hill) p 4-2
[23] Juza J and Sifner O 1977 *Acta Technica CSAV* 1
[24] Street W B, Sagan L S and Stavely L A K 1973 *J. Chem. Thermodyn.* 5 633
[25] Theeuwes F and Bearman R J 1970 *J. Chem. Thermodyn.* 2 507
[26] Theeuwes F and Bearman R J 1970 *J. Chem. Thermodyn.* 2 501
[27] Amey R L and Cole R H 1964 *J. Chem. Phys.* **40** 146 The value of the CM function reported by these authors must be corrected because they used an incorrect density of the liquid near the triple point to convert the measured dielectric constant to the Clausius–Mossotti function. The corrected value of the CM function is thus 10.03×10^{-3} l mol^{-1} near the triple point
[28] Marcoux J 1970 *Can. J. Phys.* **48** 244
[29] Smith R A 1959 *Semiconductors* (Cambridge: Cambridge University Press) p 119
[30] Huang S S S and Freeman G R 1978 *J. Chem. Phys.* **68** 1355 A table corresponding to the data used in figure 1 is given Jacobsen F M, Gee N and Freeman G R 1986 *Phys. Rev.* A **34** 2329, but the densities that correspond to the stated temperatures disagree with those given in [23–26]. The density of the data plotted in figure 1 has been recalculated using the equation for the density along the coexistence line given in [23–26]
[31] Ascarelli G 1986 *Phys. Rev.* B **34** 4278 The point corresponding to the mobility maximum in figure 7 of this reference is in error due to a numerical mistake associated with the phonon scattering
[32] Miller L S, Howe S and Spear W E 1968 *Phys. Rev.* **166** 871
[33] Huang S S S and Freeman G R 1981 *Phys. Rev.* A **24** 714
[34] Shinsaka K, Codoma M, Srinthanratana T, Yamamoto M and Hatano Y 1988 *J. Chem. Phys.* **88** 7529
[35] Jacobsen F M, Gee N and Freeman G R 1986 *Phys. Rev.* A **34** 2329
[36] Muñoz R C and Ascarelli G 1983 *Phys. Rev. Lett.* **51** 215
[37] Holroyd R and Cipollini N E 1978 *J. Chem. Phys.* **69** 502
[38] Asaf U, Reininger R and Steinberger I T 1983 *Phys. Lett.* **100** 363
[39] De Gennes P D 1985 *Rev. Mod. Phys.* 57 827
[40] Israelachvili J N 1982 *Adv. Colloid Interface Sci.* **16** 31 and references therein
[41] Bennet G T, Coffman R B and Thompson J C 1987 *J. Chem. Phys.* **87** 7242
[42] Eigler D M, Weiss P S, Schweiwer E K and Lang N D 1991 *Phys. Rev. Lett.* **66** 1189
[43] Ascarelli G and Nakanishi H 1990 *J. Physique* **51** 341
[44] Buckman S J, Elford M T and Newman D S 1987 *J. Phys. B: At. Mol. Phys.* **20** 5175
[45] Hake R D Jr. and Phelps A V 1967 *Phys. Rev.* **158** 70
[46] Ascarelli G 1990 *Non Equilibrium Effects in Ion and Electron Transport* ed J W Gallagher, D F Hudson, E E Kunhardt and R J Van Brunt (New York: Plenum) p 291
[47] Liou Y J, Hudson R A, Wonnel S K and Slifkin L M 1990 *Phys. Rev.* B **41** 10481
[48] Altshuler B L, Gefen Y and Imry Y 1991 *Phys. Rev. Lett.* **66** 88
[49] Yoshino K, Sowada U and Schmidt W F 1976 *Phys. Rev.* A **14** 438